Inorganic Chemistry

Article

pubs.acs.org/IC

Modulating Stepwise Photochromism in Platinum(II) Complexes with Dual Dithienylethene−Acetylides by a Progressive Red Shift of Ring-Closure Absorption

Bin Li,[†] Hui-Min Wen,[†] Jin-Yun Wang,[†] Lin-Xi Shi,[†] and Zhong-Ning Chen*[,†,‡]

[†]State Key Laboratory of Structural Chemistry, Fujian Institute of Research on the Structure of Matter, Chinese Academy of Sciences, Fuzhou, Fujian 350002, China

[‡]State Key Laboratory of Organometallic Chemistry, Shanghai Institute of Organic Chemistry, Chinese Academy of Sciences, Shanghai 200032, China

Supporting Information

ABSTRACT: To modulate stepwise photochromism by shifting ring-closure absorption of the dithienylethene (DTE) moiety, *trans*-$Pt(PEt_3)_2(C{\equiv}C\text{-}DTE)_2$ [C≡C-DTE = L1o (**1oo**), L2o (**2oo**), L3o (**3oo**), and L4o (**4oo**)] and *cis*-$Pt(PEt_3)_2(L4o)_2$ (**5oo**) with two identical DTE−acetylides were elaborately designed. With the gradual red shift of ring-closure absorption for L1c (441 nm) → L2c (510 nm) → L3c (556 nm) → L4c (602 nm), stepwise photochromism is increasingly facilitated in *trans*-$Pt(PEt_3)_2(C{\equiv}C\text{-}DTE)_2$ following **1oo** → **2oo** → **3oo** → **4oo**. The conversion percentage of singly ring-closed **2co**−**4co** to dually ring-closed **2cc**−**4cc** at the photostationary state is progressively increased in the order **1cc** (0%) → **2cc** (18%) → **3cc** (67%) → **4cc** (100%). Compared with trans-arranged **4oo**, stepwise photochromism in the corresponding cis-counterpart **5oo** is less pronounced, ascribed to either direct conversion of **5oo** to **5cc** or rapid conversion of **5co** to **5cc**. The progressively facile stepwise photocyclization following **2oo** → **3oo** → **4oo** is reasonably interpreted by gradually enhanced transition character involving LUMO+1, which is the only unoccupied frontier orbital responsible for further photocyclization of singly ring-closed **2co**−**4co**.

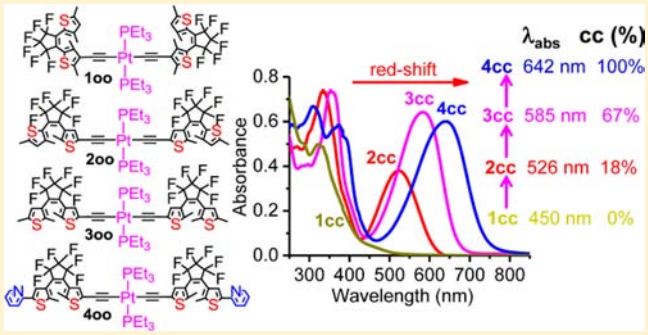

INTRODUCTION

Photochromic systems with the dithienylethene (DTE) moiety have been widely applied in photonics, electronics, and material and biological fields.[1−3] Thermal stability, fatigue resistance, and convenient functionalization make them excellent components for memories and switches at the molecular level. On the one hand, the incorporation of DTE to a suitable metal ion through coordination bonds is a feasible approach for improving the photochromic performance as well as modulating intramolecular electronic and magnetic interactions.[4−22] On the other hand, because the integrated entities with two or more DTE units are useful in achieving multiswitchable, multicolor, and multistate systems, multiphotochromism is highly promising for multifrequency optical memories to store more information in a single molecule as well as build complex devices.[23]

Nevertheless, achieving stepwise or selective photochromism in a multi-DTE system to access all of the possible ring-opened/closed isomers is quite challenging because ring closure in one DTE moiety must be well communicated with other ring-opened photochromes, while still retaining the photochemical reactivity of each DTE unit. On the one hand, ring closure at one DTE moiety usually impedes further photoreactivity of other DTE units because of rapid intercomponent energy transfer from the ring-opened moiety to the ring-closed one so that only partially ring-closed forms could be obtained, whereas a fully ring-closed isomer is normally inaccessible.[24−32] On the other hand, for electronically isolated systems with complete independence for each DTE unit, irradiation with UV light usually induces simultaneous photocyclization for each DTE moiety so that mixed ring-closed/opened forms could not be accessed.[33−40] In this case, simultaneous ring closure results simply in cumulative absorption spectra of multi-DTE units without emergent features or spectral shifts.

To achieve stepwise photochromism in a molecule combined with multi-DTE moieties, it is necessary to facilitate electronic interaction but minimize energy transfer from ring-opened DTE moieties to ring-closed ones by the judicious selection of a suitable connector to space DTE units while retaining the electronic communication between them. 1,4-Phenylene,[41] dimethylsilyl,[42] or 1,3,5-trivinylphenylene[43] seems to be a suitable spacer for stepwise photochromism when multi-DTE units are proximately connected. Complexation of multi-DTE

Received: June 22, 2013
Published: October 14, 2013

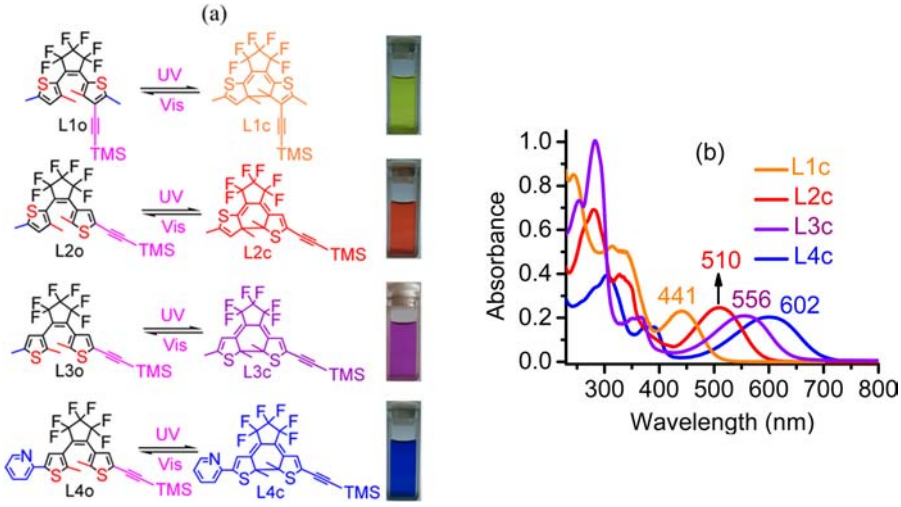

Figure 1. (a) Photochromic reactions and color changes of L1o−L4o. (b) UV−vis absorption spectra of L1c−L4c in CH_2Cl_2.

moieties with a metal ion is an alternative approach for stepwise photochromism,[44−46] although it is undetectable in most cases.[30−32,39] When two DTE units are bound to an Au^{I},[44] Pt^{II},[45] or $Ru^{II/III}$[46] through bis(σ-acetylide) bonds, distinct stepwise photochromism has been indeed observed, in which ring closure at one DTE unit does not significantly reduce the photochemical reactivity at the other. It is worth mentioning that when two DTE units are bound to a $Ru(dppe)_2$ [dppe = 1,2-bis(diphenylphosphino)ethane] moiety through the formation of two Ru−acetylide σ bonds, distinct stepwise photochromism can be achieved by different stimuli such as light irradiation or electrochemical oxidation/reduction.[38,46] With a theoretical computational approach, it has been proposed by Jacquemin and co-workers that only the unoccupied frontier orbitals that contribute to UV absorption in the mixed ring-opened and -closed isomers are responsible for further photocyclization toward the formation of a fully ring-closed form.[23]

Apart from the character of the linker that spaces the photochromic units, it is likely that DTE itself plays a crucial role in achieving stepwise photochromism. With this in mind, we are devoted to modulating ring-closure absorption of the DTE moiety by modifying the π-conjugated system. When cyclopentene is integrated with thienyl in different positions and 2-pyridyl is introduced, DTE−ethynyl ligands L1o−L4o (Figure 1) are elaborately designed, which show a progressive red shift of ring-closure absorption in the order L1c (441 nm) → L2c (510 nm) → L3c (556 nm) → L4c (602 nm). Remarkably, with the progressive red shift of ring-closure absorption in DTE−ethynyl ligands, stepwise photochromism is increasingly pronounced in the corresponding *trans*-$Pt(PEt_3)_2(C{\equiv}C\text{-}DTE)_2$, following **1oo** → **2oo** → **3oo** → **4oo** (100%) (Scheme S1 in the Supporting Information, SI). Furthermore, *trans*-platinum(II) complex **4oo** is more favorable for stepwise photochromism than the cis-oriented counterpart **5oo**.

■ RESULTS AND DISCUSSION

Considering that ring-closure absorption of DTE is quite sensitive to the combining position of the thienyl moiety to the cyclopentene moiety, the DTE−ethynyl ligands L1−L4 with various π-conjugated systems are elaborately designed. When 2-thienyl is attached to the cyclopentene moiety, ring-closure absorption usually shows a distinct blue shift relative to the DTEs having 3-thienyl.[47] L1o with two 2-thienyl moieties exhibits ring-closure absorption centered at 441 nm. By comparison, ring-closure absorption of L2o having one 2-thienyl and one 3-thienyl shows a distinct red shift to 510 nm. Ring-closure absorption of L3o with two 3-thienyl moieties is further red-shifted to 556 nm. Compared with that of L3o, ring-closure absorption of L4o is distinctly red-shifted to 602 nm upon introduction of 2-pyridyl. As depicted in Figure 1, ring-closure absorption maxima occur at 441, 510, 556, and 602 nm upon irradiation of L1o−L4o at 365 nm to the photostationary state (PSS), with the colorless solution turning yellow, red, purple, and blue, respectively. It is worth mentioning that the counterpart of L1o with 5-(trimethylsilyl)ethynyl instead of 4-(trimethylsilyl)ethynyl shows inactive photoreactivity. Photochemical quantum yields and conversion percentages of L1o−L4o at the PSS are summarized in Table 1.

Table 1. Photochemical Quantum Yields and Conversion Percentages at the PSS for L1o−L4o[a]

	Φ_{o_c}[c]	Φ_{c_o}[d]	conversion at the PSS (%)[b]
L1o	0.62 (→L1c)	0.048 (→L1o)	58
L2o	0.38 (→L2c)	0.86 (→L2o)	48
L3o	0.22 (→L3c)	0.082 (→L3o)	45
L4o	0.40 (→L4c)	0.027 (→L4o)	>95

[a]Data obtained with an uncertainty of ±10%. [b]Conversion percentages measured by NMR spectroscopy. [c]Data obtained by irradiation at 365 nm. [d]Data obtained by visible-light irradiation at >460 nm.

trans-$Pt(PEt_3)_2(C{\equiv}C\text{-}DTE)_2$ complexes **1**−**4** were prepared by the reaction of *trans*-$Pt(PEt_3)_2Cl_2$ with 2 equiv of L1o−L4o through CuI-catalyzed Pt−acetylide bonding formation. Similarly, the *cis*-$Pt(PEt_3)_2(L4o)_2$ complex **5** was accessible by the same synthetic procedure using *cis*-$Pt(PEt_3)_2Cl_2$ and L4o. It is noteworthy that cis-oriented complex **5** is sufficiently stable under UV−vis irradiation without conversion to the trans isomer or degradation.

UV−Vis Absorption Spectral Studies. Complexes **1oo**−**5oo** exhibit intense absorption bands at ca. 260−360 nm because of intraligand (IL) transitions within two DTE−acetylides together with absorption shoulder bands tailing to

450 nm, arising mainly from 5d(Pt) → π^*(C≡C-DTE/PEt_3) metal-to-ligand charge-transfer (MLCT) and ligand-to-ligand charge-transfer (LLCT) states from one ring-opened C≡C-DTE to another, as revealed by time-dependent density functional theory (TD-DFT) studies (vide infra).

When **1oo** in CH_2Cl_2 was irradiated under UV light at 365 nm, the intense absorptions at 288 and 332 nm decreased gradually, whereas a new shoulder band at ca. 450 nm occurred because of photocyclization of L1o to L1c (Figure 2a).

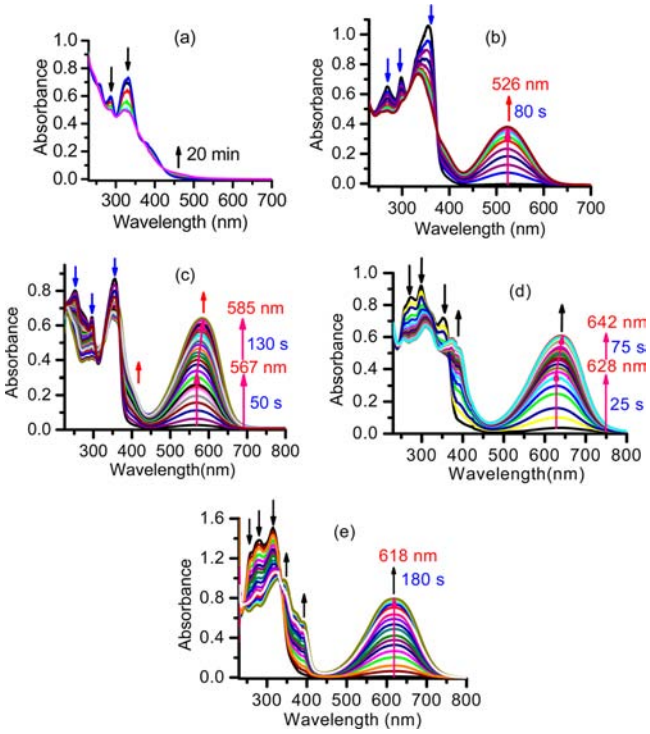

Figure 2. UV−vis absorption spectral changes of **1oo** (a), **2oo** (b), **3oo** (c), **4oo** (d), and **5oo** (e) in a CH_2Cl_2 solution at ambient temperature upon irradiation at 365 nm.

Nevertheless, the absorbance at ca. 450 nm is very low even if the solution was irradiated at 365 nm for quite a long time. The quite low ring-closure conversion percentage (<5%; Table 2) and photocyclization quantum yield (0.004) arise likely from the overlapping of ring-closure absorption (ca. 450 nm) with a low-energy MLCT band. The possible back energy transfer from ring-closing ^{1}IL/^{3}IL to ^{1}MLCT/^{3}MLCT states makes the ring-closure reaction at L1o inefficient.[16,17a,20]

Table 2. Conversion Maxima and Conversion Percentages at the PSS for 1−5[a]

	conversion maximum	contents at the PSS[b]
1oo	5% (→**1co**)	**1oo** (95%), **1co** (5%)
2oo	80% (→**2co**)	**2oo** (12%), **2co** (70%), **2cc** (18%)
3oo	60% (→**3co**) 67% (→**3cc**)	**3co** (33%), **3cc** (67%)
4oo	49% (→**4co**) 100% (→**4cc**)	**4cc** (100%)
5oo	19% (→**5co**) 100% (→**5cc**)	**5cc** (100%)

[a]Data obtained with an uncertainty of ±10%. [b]Conversion percentages measured by NMR spectroscopy.

Upon irradiation of **2oo** at 365 nm, while the intense absorption bands at 269, 298, and 355 nm gradually decreased, the ring-closure absorption band centered at 525 nm (Figure 2b) occurred and progressively enhanced in the intensity. The reaction reached the PSS in 80 s, with the colorless solution turning red. Because of the low conversion percentage to **2cc** (18%) at the PSS as demonstrated by NMR studies (vide infra), a distinct shift of the ring-closure band was unobserved with the ongoing stepwise photocyclization **2oo** → **2co** → **2cc**.

When a CH_2Cl_2 solution of **3oo** was irradiated at 365 nm, the intense absorption bands at 252, 296, and 355 nm reduced gradually. Meanwhile, the ring-closure absorption maximum occurred at 567 nm (Figure 2c), which showed a gradual red shift to 585 nm at the PSS, with the colorless solution becoming purple. Such a distinct red shift of ring-closure absorption demonstrated unambiguously that stepwise photocyclization occurred indeed through **3oo** → **3co** → **3cc**. A 543 cm^{-1} (18 nm) red shift of the ring-closure absorption upon first the formation of **3co** (567 nm) and then **3cc** (585 nm) is ascribed to the increased π system in the latter. Conversely, when the solution at the PSS was irradiated with light at >460 nm (Figure S1 in the SI), the reversed UV−vis absorption spectral changes were observed with stepwise cycloreversion reactions **3cc** → **3co** → **3oo**. Moreover, the reversibility of the photochromic behavior on complex **3oo** has been studied. As shown in Figure 3, **3oo** shows good reversibility in its photochromic behavior, with no apparent deterioration of the intensity of the absorption maximum at 585 nm upon repeating over at least six cycles.

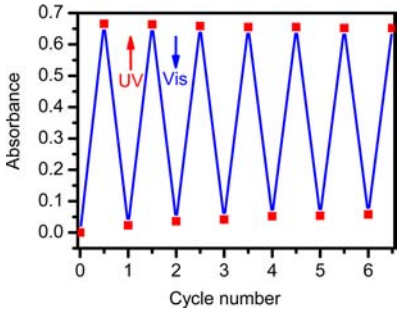

Figure 3. UV−vis absorbance changes of complex **3** at 585 nm upon alternate excitation at 365 and >460 nm over six cycles at room temperature.

When **4oo** in CH_2Cl_2 was irradiated at 365 nm, the ring-closure absorption maximum occurred first at 628 nm and then red-shifted progressively to 642 nm (Figure 2d), with the colorless solution turning blue. As found in **3oo**, an obvious red shift (14 nm) of the ring-closure absorption maximum from 628 to 642 nm is clearly indicative of the occurrence of stepwise photocyclization reactions **4oo** → **4co** → **4cc**. Obviously, relative to that in singly ring-closed **4co** (628 nm), ring-closure absorption in dually ring-closed **4cc** (642 nm) is distinctly red-shifted because of the enhanced π system upon conversion of both L4o to ring-closed L4c.

Upon irradiation of **5oo** in CH_2Cl_2 at 365 nm, while intense absorption bands at 258, 280, and 315 nm decreased gradually, three new bands at 345, 390, and 618 nm occurred (Figure 2e). They were progressively enhanced in intensity until to the PSS, but a distinct red shift of ring-closure absorption (618 nm) was unobserved. The same ring-closure absorption for both **5co** and **5cc** is likely due to the localized orbital distribution at one of the two L4c in **5cc**, in striking contrast to delocalization over the whole molecule in the trans counterpart **4cc** from TD-DFT studies. Relative to that of free L4c (602 nm), ring-closure

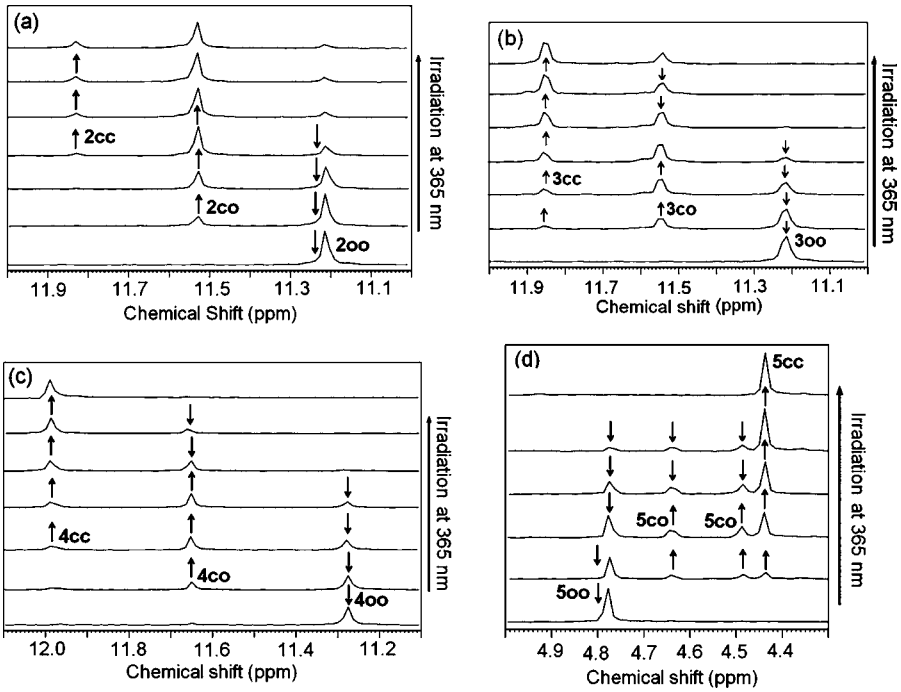

Figure 4. ^{31}P NMR spectral changes of **2oo** (a), **3oo** (b), **4oo** (c), and **5oo** (d) in $CDCl_3$ under UV-light irradiation at 365 nm to the PSS.

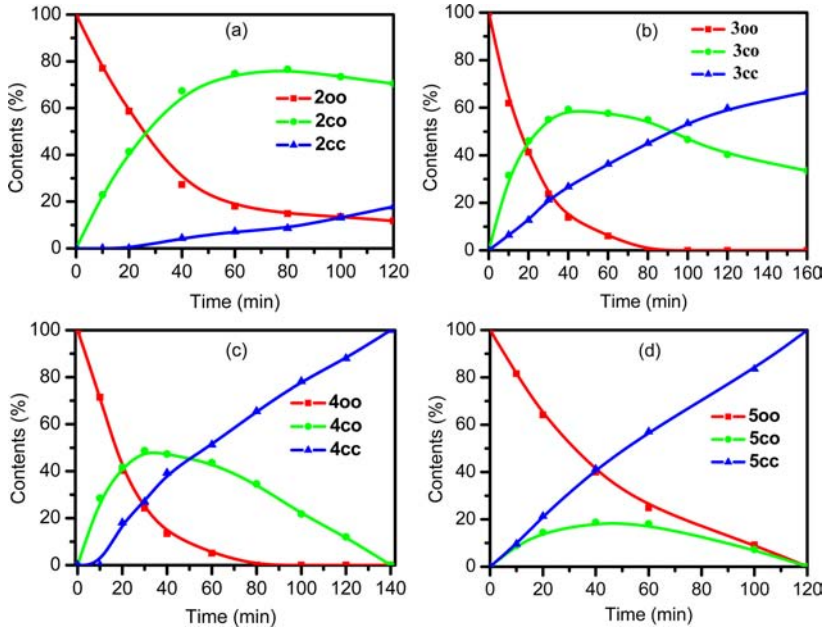

Figure 5. Relative content changes of **2oo** (a), **3oo** (b), **4oo** (c), and **5oo** (d) in $CDCl_3$ under UV-light irradiation at 365 nm to the PSS.

absorption of **4cc** (642 nm) shows more red shift than that of **5cc** (618 nm), further implying a better π-delocalized system for **4cc** than for cis-arranged **5cc**.

NMR Spectral Studies. When **1oo** in $CDCl_3$ was irradiated at 365 nm, the ^{1}H NMR spectral signal of the thienyl proton (Figure S2 in the SI) at 6.49 ppm (H_{1o}) weakened slightly, whereas a new signal at 5.52 ppm (H'_{1c}) occurred. On the other hand, the ^{31}P NMR signal (Figure S3 in the SI) at 10.98 ppm reduced slightly, whereas a new signal occurred at 11.31 ppm upon the formation of singly ring-closed **1co**. Because the new signals in both ^{1}H and ^{31}P NMR spectra were not obviously enhanced upon continued irradiation at 365 nm for 1 day, photocyclization in **1oo** ($\Phi_{o\rightarrow c}$ = 0.004) is very inefficient. At the PSS, the conversion percentage to **1co** is less than 5%, coinciding with the UV−vis absorption spectral studies. Conversion maxima and conversion percentages at the PSS for **1oo**−**5oo** are summarized in Table 2.

Upon irradiation of **2oo** in $CDCl_3$ at 365 nm, while the ^{1}H NMR spectral signals (Figure S4 in the SI) at 6.51 and 6.77 ppm due to the thienyl protons weakened gradually, two new signals at 5.28 and 6.00 ppm occurred and enhanced increasingly because of conversion of L2o to L2c. The proton signals of three CH_3 in **2oo** (Scheme S2 and Figure S4 in the SI) occurred at 2.44 (methyl a), 1.85 (methyl c), and 1.70 ppm (methyl b). Upon irradiation at 365 nm, the three methyl signals gradually attenuated, with the occurrence of four new

low-field-shifted signals at 2.01 (methyl a′), 1.86 (methyl f′), 1.75 (methyl c′), and 1.64 ppm (methyl b′) following L2o → L2c conversion.

Upon irradiation of **2oo** at 365 nm, while the P signal at 11.21 ppm reduced gradually, a new signal occurred first at 11.53 ppm (Figure 4a), followed by the occurrence of another new peak at 11.83 ppm, ascribable to the stepwise formation of **2co** first and then **2cc**. At the PSS, the P signal integral ratio of **2oo**, **2co** and **2cc** suggests the presence of 12% of **2oo**, 70% of **2co** and 18% of **2cc** (Figure 5a).

When **3oo** in $CDCl_3$ was irradiated at 365 nm, the ^{1}H NMR spectral signals (Figure S5 in the SI) at 6.78 (thienyl H_{2o}) and 6.70 ppm (thienyl H_{1o}) weakened gradually. In contrast, three new signals at 6.79 (H'_{2o}), 6.69 (H'_{1o}), and 5.98 ppm (H'_{2c}/H'_{1c}) occurred following photocyclization **3oo** → **3co** (Scheme 1). Upon continued irradiation at 365 nm to the PSS, while the

Scheme 1. Stepwise Photochromic Reactions for 3oo−5oo

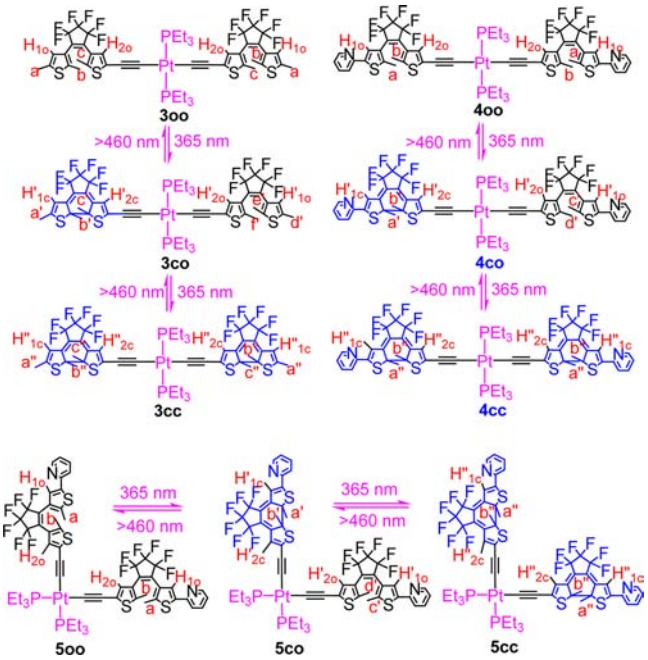

signals at 6.79 (H'_{2o}) and 6.69 ppm (H'_{1o}) decreased gradually, the signal at 5.98 ppm (H''_{1c}/H''_{2c}) increased continually, implying a further conversion of **3co** to **3cc**. The signals of the CH_3 protons in **3oo** occurred at 2.41 (methyl a), 1.85 (methyl b), and 1.79 ppm (methyl c) (Figure S6 in the SI). Upon irradiation of **3oo** at 365 nm, the three methyl signals were gradually attenuated with the occurrence of four new low-field-shifted signals at 2.17 (methyl a′), 2.06 (methyl b′), 2.05 (methyl c′), and 1.80 ppm (methyl d′) because of **3oo** → **3co** conversion (Scheme 1). Further irradiation at 365 nm resulted in a gradual reduction for both sets of methyl signals for **3oo** and **3co**, whereas three signals at 2.17, 2.06, and 2.05 ppm were gradually enhanced because of further photocyclization of the second DTE to produce **3cc**.

Stepwise photochromic reactions of **3oo** were unambiguously supported by ^{31}P NMR spectral studies (Figure 4b). Upon irradiation of **3oo** at 365 nm, while the P signal at 11.22 ppm reduced gradually and vanished finally, a new P signal was first observed at 11.54 ppm because of the formation of **3co**. Continued irradiation at 365 nm indicated that the P signal of **3co** (11.54 ppm) decreased gradually, whereas another new peak appeared at 11.85 ppm, ascribed to further conversion of **3co** to **3cc**. The contents of **3oo**, **3co**, and **3cc** against the irradiation time are depicted in Figure 5b. It is unambiguously revealed that **3oo** is first converted to **3co** and then to **3cc**. At the PSS, the P signal integral ratio between **3co** and **3cc** suggests the presence of 33% **3co** and 67% **3cc**.

Upon irradiation of **4oo** in $CDCl_3$ at 365 nm, while the ^{1}H NMR spectral signals (Figure 6) at 7.60 (H_{1o}) and 6.78 ppm

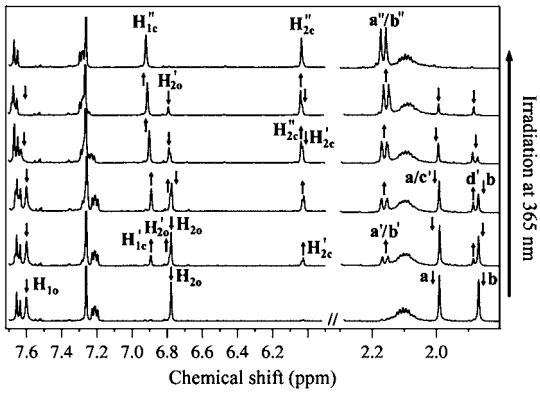

Figure 6. ^{1}H NMR spectral changes of **4oo** in $CDCl_3$ upon irradiation at 365 nm to the PSS.

(H_{2o}) weakened gradually, four new signals at 7.61 (H'_{1o}), 6.79 (H'_{2o}), 6.89 (H'_{1c}), and 6.02 ppm (H'_{2c}) occurred following photocyclization **4oo** → **4co** (Scheme 1). Upon continued irradiation at 365 nm to the PSS, while the signals at 7.61 (H'_{1o}), 6.79 (H'_{2o}), 6.89 (H'_{1c}), and 6.02 ppm (H'_{2c}) decreased gradually and finally vanished, two new signals at 6.92 (H''_{1c}) and 6.04 ppm (H''_{2c}) were observed, implying a further conversion of **4co** to **4cc**. The CH_3 signals in **4oo** occurred at 1.99 (methyl a) and 1.87 ppm (methyl b) (Figure 6). Upon irradiation at 365 nm, while the two methyl signals were gradually attenuated, two new low-field-shifted signals at 2.17 (methyl a′) and 2.15 ppm (methyl b′) occurred together with another two new methyl signals at 2.00 (methyl c′) and 1.89 ppm (methyl d′) with a slight low-field shift relative to methyl a (1.99 ppm) and b (1.87 ppm), suggesting the occurrence of **4oo** → **4co** conversion. Further irradiation at 365 nm resulted in a gradual reduction for both sets of methyl signals of **4oo** and **4co**, whereas another two methyl signals at 2.18 (methyl a″) and 2.16 ppm (methyl b″) occurred because of further conversion of **4co** to **4cc**.

As depicted in Figure 4c, the stepwise ring-closure reactions **4oo** → **4co** → **4cc** were unambiguously supported by ^{31}P NMR spectral studies. Upon irradiation of **4oo** at 365 nm, with the gradual decrease and vanishing of the P signal at 11.27 ppm, a new P signal occurred progressively at 11.65 ppm because of the formation of **4co**. Upon further irradiation at 365 nm, the P signal at 11.65 ppm (**4co**) decreased gradually and finally vanished, whereas another new peak occurred at 11.98 ppm because of conversion of **4co** to **4cc**. At the PSS, only one P signal at 11.98 ppm was observed, suggesting the presence of 100% of **4cc** (Figure 5c).

Upon irradiation of **5oo** at 365 nm, the ^{1}H NMR spectral studies indicated that the thienyl proton signals (Figure S7 in the SI) at 7.49 (H_{1o}) and 6.98 ppm (H_{2o}) gradually weakened, whereas four new signals at 7.50 (H'_{1o}), 6.98 (H'_{2o}), 6.88 (H'_{1c}), and 6.23 ppm (H'_{2c}) increasingly occurred because of photocyclization **5oo** → **5co** (Scheme 1). Upon continued

irradiation at 365 nm, while the signals at 7.50 (H'_{1o}), 6.98 (H'_{2o}), 6.88 (H'_{1c}), and 6.24 ppm (H'_{2c}) decreased gradually and vanished at the PSS, two new signals at 6.89 (H''_{1c}) and 6.23 ppm (H''_{2c}) appeared, implying further conversion of **5co** to **5cc**. The signals of the CH_3 protons in **5oo** appeared at 1.97 (methyl a) and 1.85 ppm (methyl b) (Figure S7 in the SI). Upon irradiation at 365 nm, the two methyl signals were gradually attenuated with the occurrence of two low-field-shifted signals at 2.16 (methyl a′) and 2.15 ppm (methyl b′) together with another two new methyl signals at 1.98 (methyl c′) and 1.87 ppm (methyl d′) due to **5oo** → **5co** conversion (Figure S7 in the SI). Further irradiation at 365 nm resulted in a gradual reduction for both sets of methyl signals of **5oo** and **5co**, whereas two new methyl signals at 2.17 (methyl a″) and 2.16 ppm (methyl b″) were observed because of the further formation of **5cc**.

Upon irradiation of **5oo** in $CDCl_3$ at 365 nm, while the P signal at 4.78 ppm decreased gradually and vanished finally, three new signals occurred at 4.64, 4.49, and 4.44 ppm (Figure 4d). Because further irradiation at 365 nm induced the P signals at 4.64 and 4.49 ppm to decrease gradually and vanish at the PSS, both signals are reasonably ascribed to **5co**. In contrast, the signal at 4.44 ppm, which was gradually increased with irradiation and was the only signal at the PSS, is assignable to **5cc**. The occurrence of only one P signal at 4.44 ppm suggests the presence of 100% of **5cc** (Figure 5d) at the PSS.

Upon UV-light irradiation of **5oo**, the P signals due to **5co** and **5cc** were synchronously observed (Figure 4d). Because the conversion maximum of **5co** was only 19% (Figure 5d), much lower than that of the trans counterpart **4co** (49%), it is likely that, to some extent, **5oo** could directly convert to **5cc** through simultaneous photocyclization at both DTE units, as found for electronically isolated systems with complete independence for each DTE unit,[33−40] resulting simply in cumulative absorption spectra of dual-DTE units without any spectral shift (Figure 2e). Another possibility is that **5co** → **5cc** conversion is much faster than that in the trans counterpart **4co** → **4cc**.

IR Spectral Studies. The IR bands of **1oo**−**5oo** due to the C≡C stretching mode occurred at 2092−2107 cm^{-1} in a CH_2Cl_2 solution. Upon irradiation of **1oo**−**5oo** (Figures S8−S12 in the SI) at 365 nm, an obvious red shift (20−30 cm^{-1}) to lower wavenumber was always observed, ascribed to the increased π system upon photocyclization at the DTE units so that a π electron of the acetylides is largely delocalized to the whole coordination system, thus attenuating C≡C bonding. Particularly, the ν(C≡C) frequency exhibits a progressive decrease with stepwise ring-closure reactions **3oo** (2092 cm^{-1}) → **3co** (2076 cm^{-1}) → **3cc** (2072 cm^{-1}) and **4oo** (2092 cm^{-1}) → **4co** (2074 cm^{-1}) → **4cc** (2069 cm^{-1}).

Electrochemical Studies. Complexes **1oo**−**5oo** (Table 3) exhibit an irreversible Pt-based oxidation wave at 1.47−1.54 V together with an irreversible DTE-centered wave at 1.13−1.24 V. Upon irradiation of **1oo**−**5oo** (Figures S13−S17 in the SI) at 365 nm to the PSS, the oxidation potentials of both Pt- and DTE-centered waves were distinctly less anodic because of the enhanced π-electron density with photocyclization at both DTE units. Particularly, the presence of two successive DTE-based oxidation waves at 0.82 and 0.96 V for **3cc** and 0.82 and 0.95 V for **4cc** suggests that moderate electron interaction is likely mediated between two ring-closed DTE units across the *trans*-$Pt(PEt_3)_2$ spacer.[48] Such an electronic communication between two identical L3c in **3cc** ($\Delta E_{1/2}$ = 0.14 V) or L4c in **4cc** ($\Delta E_{1/2}$ = 0.13 V) is comparable to that between two Fc in *trans*-$[Pt(C_6F_5)_2(C{\equiv}C{-}Fc)_2]^{2-}$ ($\Delta E_{1/2}$ = 0.14 V)[49] across the *trans*-$Pt(C_6F_5)_2$ spacer but higher than that in *trans*-$Pt(PPh_3)_2(C{\equiv}C{-}Fc)_2$ ($\Delta E_{1/2}$ = 0.08 V).[50] In contrast, distinct DTE-based redox splitting was unobserved for cis-arranged **5cc**. As revealed by TD-DFT studies, the highest occupied molecular orbitals (HOMOs) and lowest unoccupied molecular orbitals (LUMOs) in trans complex **4cc** (Figure S29 in the SI) are delocalized over the whole coordinated system, while those in the cis counterpart **5cc** (Figure S32 in the SI) are localized on one of the two L4c, which is unfavorable for electronic communication.

Table 3. Electrochemical Data of Complexes 1−5 versus Ag/AgCl in 0.1 M (Bu^n_4N)(PF_6)−Dichloromethane Solutions[a]

compound	E_a(Pt-based)[b]	E_a(DTE-based)[c]
1oo	1.48	1.24
1co	1.45	0.83
2oo	1.52	1.17
2co	1.51	0.90
3oo	1.54	1.17
3cc	1.53	0.82, 0.96
4oo	1.49	1.17
4cc	1.12	0.82, 0.95
5oo	1.47	1.13
5cc	1.10	0.78

[a]Potential data in volts vs Ag/AgCl. [b]Anodic potential due to a Pt-centered oxidation process. [c]Anodic potential due to oxidation of DTEs.

Computational Studies. TD-DFT calculations were performed on **1oo**/**1co** to **5oo**/**5co**/**5cc** (Tables S1−S15 in the SI). The UV absorption bands of **1oo**−**4oo** with electron promotion from HOMO to LUMO/LUMO+*n* are mainly characteristic of DTE−acetylide IL character, mixed with moderate MLCT (Pt → DTE−acetylide) and LLCT states from one DTE−acetylide to the other. For **5oo**, the lowest energy of UV absorption due to HOMO → LUMO+4 is featured with a DTE−acetylide IL state mixed with minor DTE−acetylide → PEt_3 LLCT character.

The low-energy absorption of **2co**−**5co** is typical of IL transition localized on the ring-closed DTE because of electron promotion from the HOMO to LUMO with an intense oscillator strength (>0.60). In contrast, ring-closure absorption of **1co** due to HOMO → LUMO+1 displays a very weak oscillator strength (0.07), coinciding with the quite low photocyclization efficiency of **1oo** with less than 5% conversion to **1co**.

It has been proposed that only the unoccupied frontier orbitals contributing to the UV absorption bands participate in photocyclization.[23,45b] For **2oo**−**5oo** species, both LUMO and LUMO+1 are responsible for ring-closure reaction. For singly ring-closed **2co**−**5co** species, the LUMO is generally localized on the ring-closed DTE unit, which is irrelevant with further photocyclization at the other ring-opened DTE moiety. Instead, LUMO+*n* that exhibit good bonding character and significant density at the reactive C atoms for the to-be-formed C−C bond in the ring-opened DTE moiety[23] are mostly responsible for further ring closure of **2co**−**5co** to produce **2cc**−**5cc**. In fact, LUMO+1 represents the only photochromism-favorable orbital that is mainly resident on the ring-opened DTE moiety in **2co**−**5co**.

As depicted in Figure 7, although LUMO+1, LUMO+2, and LUMO+3 of **3co** are resident on the ring-opened DTE unit to

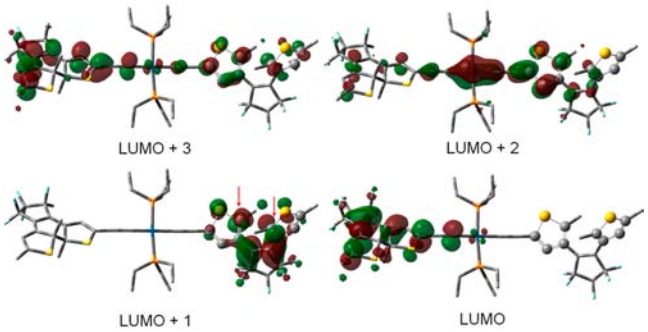

Figure 7. Plots of unoccupied orbitals involved in the absorption transitions for singly ring-closed **3co**. The red and green regions donate different phases. The reactive C atoms in LUMO+1 responsible for further ring closure are indicated by arrows.

exhibit significant electronic density at the reactive C atoms, only LUMO+1 is phase-matching with bonding character and favorable for photocyclization through formation of the C−C bond.

For **2co** (Table S5 in the SI), because HOMO−2 → LUMO +1 with 11% contribution represents the only UV absorption (S_7 at 335 nm) transition involving LUMO+1, a low conversion yield of **2co** → **2cc** (18% at the PSS) is reasonable. For **3co** (Table S8 in the SI), several UV absorption transitions involving LUMO+1, including HOMO−1 → LUMO+1 (13%), HOMO−8 → LUMO+1 (9%), HOMO−8 → LUMO+1 (35%), and HOMO−6 → LUMO+1 (18%), induce much more conversion of **3co** to **3cc** (67% at the PSS) than that of **2co** to **2cc** (18% at the PSS). The 100% conversion of **4co** to **4cc** or **5co** to **5cc** is correlated to three or two significant UV absorption transitions involving LUMO+1, including HOMO−8 → LUMO+1 (42%), HOMO−5 → LUMO+1 (27%), and HOMO−6 → LUMO+1 (12%) for **4co** (Table S11 in the SI) and HOMO−7 → LUMO+1 (57%) and HOMO−4 → LUMO+1 (15%) for **5co** (Table S14 in the SI).

Ring-closure absorption for dually ring-closed species **2cc**−**4cc** is due to electron promotion from HOMO to LUMO, whereas that for **5cc**, from HOMO−1 → LUMO and HOMO → LUMO+1. The transition energy of HOMO → LUMO reduces progressively with stepwise photocyclization, following $E_{oo} > E_{co} > E_{cc}$ for complexes **2**−**4**, coinciding with a gradual red shift of ring-closure absorption measured experimentally. For complex **5**, the transition energy follows E_{5oo} (3.6 eV) > E_{5co} (2.0 eV) = E_{5cc} (2.0 eV), coinciding with measured ring-closure absorption without a distinct red shift upon stepwise photocyclization.

■ CONCLUSIONS

L1o−L4o with progressively red-shifted ring-closure absorption were elaborately designed to modulate stepwise photochromism in platinum(II) complexes **1oo**−**5oo**. With the progressive red shift of ring-closure absorption following L1o → L2o → L3o → L4o, stepwise photocyclization is increasingly facilitated in *trans*-platinum(II) complexes following **1oo** → **2oo** → **3oo** → **4oo**. The progressively facile stepwise photocyclization following **2oo** → **3oo** → **4oo** is reasonably interpreted by TD-DFT studies, in which singly ring-closed species following **2co** → **3co** → **4co** exhibit gradually enhanced transition character involving LUMO+1, which is the only unoccupied orbital having significant electronic density at the reactive C atoms responsible for further photocyclization at the other ring-opened DTE. In contrast to distinct stepwise photochromism for **4oo** → **4co** → **4cc**, a much lower conversion maximum of cis-arranged **5co** (19%) was detected because of either rapid conversion of **5co** to **5cc** or direct conversion of **5oo** to **5cc**. As a result, *trans*-$Pt(PEt_3)_2$ as a spacer is more favorable than *cis*-$Pt(PEt_3)_2$ for stepwise photochromism because it transmits more pronounced electronic interaction. The results offer a new approach to modulating stepwise photochromism through modifying ring-closure absorption of DTE moieties apart from altering the linker.

■ EXPERIMENTAL SECTION

General Procedures and Materials. All of the synthetic procedures were carried out using Schlenk techniques and vacuum-line systems under a dry argon atmosphere. Solvents were distilled under an argon atmosphere in the presence of sodium benzophenone or calcium hydride. *cis*/*trans*-$Pt(PEt_3)_2Cl_2$, 1-(3,5-dimethyl-2-thienyl)-2-(4-bromo-3,5-dimethyl-2-thienyl)perfluorocyclopentene, 3-bromo-2-methyl-5-(trimethylsilyl)ethynylthiophene, (3,5-dimethyl-2-thienyl)-perfluorocyclopentene, (2,5-dimethyl-3-thienyl)-perfluorocyclopentene, and L4o were prepared by literature procedures.[46,47,51,52]

Synthesis of 1-(3,5-Dimethyl-2-thienyl)-2-(4-iodo-3,5-dimethyl-2-thienyl)perfluorocyclopentene. A solution of 1-(3,5-dimethyl-2-thienyl)-2-(4-bromo-3,5-dimethyl-2-thienyl)-perfluorocyclopentene (948 mg, 2 mmol) in anhydrous ether (40 mL) was cooled to −78 °C. To the solution was slowly added *n*-butyllithium (1.6 M in hexane, 1.3 mL, 2.1 mmol). After stirring for 1 h at −78 °C, a solution of iodine (1.03 g, 4 mmol) in anhydrous ether (10 mL) was added to the reaction solution. The mixture is then stirred at −78 °C for 2 h and then slowly warmed to room temperature with stirring for 16 h before the addition of a solution of aqueous sodium sulfite (30 mL). The mixture was extracted with petroleum ether three times. The combined organic layer was dried with $MgSO_4$, then filtered, and evaporated in vacuo. The product was purified by column chromatography on silica gel using petroleum ether. Yield: 70% (730 mg). ^{1}H NMR ($CDCl_3$, ppm): δ 6.52 (s, 1H), 2.46 (s, 3H), 2.45 (s, 3H), 1.80 (s, 3H), 1.72 (s, 3H). ESI-MS: m/z 522 (100%) [M^+].

Synthesis of L1o. 1-(3,5-Dimethyl-2-thienyl)-2-(4-iodo-3,5-dimethyl-2-thienyl)perfluorocyclopentene (730 mg, 1.40 mmol), tetrakis(triphenylphosphine)palladium(0) (50 mg, 0.07 mmol), and copper(I) iodide (4 mg, 20 μmol) were dissolved in triethylamine (30 mL), followed by the addition of (trimethylsilyl)acetylene (0.6 mL, 4 mmol). The reaction mixture was stirred at 70 °C overnight, which was monitored by thin-layer chromatography (TLC). The mixture was filtered, and the filtrate was then concentrated under reduced pressure. The product was purified by silica gel column chromatography using petroleum ether as the eluent to afford a yellow solid. Yield: 48% (331 mg). ^{1}H NMR ($CDCl_3$, ppm): δ 6.52 (s, 1H), 2.51 (s, 3H), 2.45 (s, 3H), 1.79 (s, 3H), 1.73 (s, 3H), 0.23 (s, 9H). ^{13}C NMR ($CDCl_3$, ppm): δ 148.1, 144.4, 142.1, 141.4, 129.4, 129.2, 123.1, 120.6, 119.7, 99.9 (C≡C), 98.4 (C≡C), 15.4 (s, CH_3), 15.3 (s, CH_3), 14.9 (s, CH_3), 14.8 (s, CH_3), 0.10 ($Si(CH_3)_3$). ESI-MS: m/z 492 (100%) [M^+]. IR (KBr): 2149 cm^{-1} (C≡C).

Synthesis of L2o. A dry THF (40 mL) solution of 3-bromo-2-methyl-5-(trimethylsilyl)ethynylthiophene (548 mg, 2 mmol) was cooled to −78 °C. To the solution was slowly added *n*-butyllithium (1.6 M in hexane, 1.3 mL, 2.1 mmol). Upon stirring at −78 °C for 30 min, (3,5-dimethyl-2-thienyl)perfluorocyclopentene (608 mg, 2 mmol) in dry THF (5 mL) was added to the solution. After further stirring at −78 °C for 2 h, dilute hydrochloric acid was added. The product was extracted with ether, dried with $MgSO_4$, and concentrated under reduced pressure. The residue was purified by silica gel column chromatography using petroleum ether as the eluent to afford the product as a pale-yellow oil. Yield: 49% (468 mg). ^{1}H NMR (400 MHz, $CDCl_3$, ppm): δ 7.21 (s, 1H), 6.52 (s, 1H), 2.44 (s, 3H), 1.90 (s, 3H), 1.68 (s, 3H), 0.25 (s, 9H). ^{13}C NMR ($CDCl_3$, ppm): δ 144.3,

143.3, 141.3, 132.6, 129.5, 125.1, 121.4, 99.7 (C≡C), 96.5 (C≡C), 15.4 (CH_3), 15.3 (CH_3), 15.2 (CH_3), −0.23 ($Si(CH_3)_3$). ESI-MS: *m/z* 479 (100%) $[M + 1]^+$. IR (CH_2Cl_2): 2149 cm^{-1} (C≡C).

Synthesis of L3o. This compound was prepared by the same synthetic procedure as that of L2o except for the use of (2,5-dimethyl-3-thienyl)perfluorocyclopentene instead of (3,5-dimethyl-2-thienyl)-perfluorocyclopentene. Yield: 65% (621 mg). ^1H NMR (400 MHz, $CDCl_3$, ppm): δ 7.22 (s, 1H), 6.69 (s, 1H), 2.41 (s, 3H), 1.84 (s, 3H), 1.83 (s, 3H), 0.24 (s, 9H). ^{13}C NMR ($CDCl_3$, ppm): δ 143.2, 139.8, 137.9, 132.3, 125.0, 124.5, 124.3, 121.4, 99.7 (C≡C), 99.4 (C≡C), 15.0 (CH_3), 14.3 (CH_3), 14.2 (CH_3), −0.30 ($Si(CH_3)_3$). ESI-MS: *m/z* 479 (100%) $[M + 1]^+$. IR (CH_2Cl_2): 2149 cm^{-1} (C≡C).

Synthesis of 1oo. *trans*-$Pt(PEt_3)_2Cl_2$ (75 mg, 0.15 mmol) and L1o (157 mg, 0.32 mmol) were dissolved in a degassed CH_2Cl_2. Tetrabutylammonium fluoride (0.1 mL, 1 M in THF) and CuI (5 mg) were then added to the solution. The reaction mixture was stirred in the dark for 1 day, in which the reaction was monitored by TLC. The product was purified by silica gel column chromatography using dichloromethane−petroleum ether (1:2, v/v) as the eluent. Yield: 65% (124 mg). ESI-MS: *m/z* 1270 (100%) $[M + 1]^+$. Anal. Calcd for $C_{50}H_{56}F_{12}P_2PtS_4$: C, 47.28; H, 4.44. Found: C, 47.52; H, 4.31. ^1H NMR (400 MHz, $CDCl_3$, ppm): δ 6.49 (s, 2H), 2.46 (s, 6H), 2.44 (s, 6H), 2.11−2.07 (m, 12H), 1.76 (s, 6H), 1.71 (s, 6H), 1.12−1.08 (m, 18H). ^{31}P NMR (161.97 MHz, $CDCl_3$, ppm): δ 10.98 (J_{Pt-P} = 2382 Hz). ^{13}C NMR ($CDCl_3$, ppm): δ 143.8, 142.6, 141.5, 141.2, 129.1, 128.3, 121.1, 118.4, 112.3 (t, J_{C-P} = 14.5 Hz, C≡C), 102.3 (C≡C), 16.3 (t, J_{C-P} = 17.5 Hz, CH_2P), 15.6 (CH_3), 15.3 (CH_3), 15.2 (CH_3), 15.0 (CH_3), 8.2 (CH_3CH_2P). IR (CH_2Cl_2): 2096 cm^{-1} (C≡C).

Synthesis of 2oo. This compound was prepared by the same synthetic procedure as that of **1oo** except for the use of L2o (153 mg, 0.32 mmol) in place of L1o. Yield: 70% (130 mg). ESI-MS: *m/z* 1242 (100%) $[M + 1]^+$. Anal. Calcd for $C_{48}H_{52}F_{12}P_2PtS_4$: C, 46.41; H, 4.22. Found: C, 46.75; H, 4.09. ^1H NMR (400 MHz, $CDCl_3$, ppm): δ 6.77 (s, 2H), 6.51 (s, 2H), 2.44 (s, 6H), 2.17−2.09 (m, 12H), 1.86 (s, 6H), 1.70 (s, 6H), 1.25−1.17 (m, 18H). ^{31}P NMR (161.97 MHz, $CDCl_3$, ppm): δ 11.21 (J_{Pt-P} = 2341 Hz). ^{13}C NMR ($CDCl_3$, ppm): δ 143.8, 141.2, 139.1, 129.3, 127.4, 127.1, 124.6, 120.7, 114.4 (t, J_{C-P} = 14.6 Hz, C≡C), 100.8 (C≡C), 16.5 (t, J_{C-P} = 17.6 Hz, CH_2−P), 15.4 (CH_3), 15.3 (CH_3), 14.2 (CH_3), 8.3 (CH_3CH_2P). IR (CH_2Cl_2): 2092 cm^{-1} (C≡C).

Synthesis of 3oo. This compound was prepared by the same synthetic procedure as that of **1oo** except for the use of L3o (153 mg, 0.32 mmol) in place of L1o. Yield: 64% (120 mg). ESI-MS: *m/z* (%) 1242 (100) $[M + 1]^+$. Anal. Calcd for $C_{48}H_{52}F_{12}P_2PtS_4$: C, 46.41; H, 4.22. Found: C, 46.80; H, 4.15. ^1H NMR (400 MHz, $CDCl_3$, ppm): δ 6.78 (s, 2H), 6.69 (s, 2H), 2.41 (s, 6H), 2.16−2.10 (m, 12H), 1.85 (s, 6H), 1.79 (s, 6H), 1.24−1.16 (m, 18H). ^{31}P NMR (161.97 MHz, $CDCl_3$, ppm): δ 11.22 (J_{Pt-P} = 2338 Hz). ^{13}C NMR ($CDCl_3$, ppm): 139.7, 138.9, 137.5, 127.3, 126.8, 124.7, 124.6, 120.7, 114.4 (t, $J_{C,P}$ = 13.9 Hz, C≡C), 100.8 (C≡C), 16.5 (t, *J*(C, P) = 17.6 Hz, CH_2P), 15.1 (CH_3), 14.3 (CH_3), 14.2 (CH_3), 8.3 (CH_3CH_2P). IR (CH_2Cl_2): 2092 cm^{-1} (C≡C).

Synthesis of 4oo. This compound was prepared by the same synthetic procedure as that of **1oo** except the use of L4o (167 mg, 0.32 mmol) in place of L1o. The product was purified by column chromatography using dichloromethane−petroleum ether (2:1, v/v) as the eluent. Yield: 75% (153 mg). ESI-MS: *m/z* 1368 (100%) $[M + 1]^+$. Anal. Calcd for $C_{56}H_{54}F_{12}N_2P_2PtS_4$: C, 49.16; H, 3.98; N, 2.05. Found: C, 49.06; H, 4.03; N, 1.98. ^1H NMR (400 MHz, $CDCl_3$, ppm): δ 8.54 (d, *J* = 4.82 Hz, 2H), 7.69 (td, J_1 = 7.92 Hz, J_2 = 1.72 Hz, 2H), 7.60 (d, *J* = 8 Hz, 2H), 7.51 (s, 2H), 7.18−7.14 (m, 2H), 6.78 (s, 2H), 2.14−2.06 (m, 12H), 1.99 (s, 6H), 1.87 (s, 6H), 1.23−1.14 (m, 18H). ^{31}P NMR (161.97 MHz, $CDCl_3$, ppm): δ 11.27 (J_{Pt-P} = 2337 Hz). ^{13}C NMR ($CDCl_3$, ppm): δ 151.7, 149.5, 144.2, 142.5, 139.0, 136.7, 127.6, 126.7, 126.0, 124.2, 124.0, 122.2, 118.5, 114.8 (t, J_{C-P} = 14.6 Hz, C≡C), 100.6 (C≡C), 16.5 (t, J_{C-P} = 17.7 Hz, CH_2P), 14.8 (CH_3), 14.4 (CH_3), 8.3 (CH_3CH_2P). IR (CH_2Cl_2): 2092 cm^{-1} (C≡C).

Synthesis of 5oo. This compound was prepared by the same synthetic procedure as that of **1oo** except for the use of *cis*-$Pt(PEt_3)_2Cl_2$ (75 mg, 0.15 mmol) and L4o (167 mg, 0.32 mmol) in place of *trans*-$Pt(PEt_3)_2Cl_2$ and L1o. Yield: 60% (123 mg). ESI-MS: *m/z* 1368 (60%) $[M + 1]^+$, 1391 (100%) $[M + Na]^+$. Anal. Calcd for $C_{56}H_{54}F_{12}N_2P_2PtS_4$: C, 49.16; H, 3.98; N, 2.05. Found: C, 49.38; H, 3.91; N, 2.01. ^1H NMR (400 MHz, $CDCl_3$, ppm): δ 8.53 (d, *J* = 4.68 Hz, 2H), 7.68 (td, J_1 = 7.72 Hz, J_2 = 1.72 Hz, 2H), 7.60 (d, *J* = 8 Hz, 2H), 7.49 (s, 2H), 7.16−7.12 (m, 2H), 6.98 (s, 2H), 2.04−1.98 (m, 12H), 1.97 (s, 6H), 1.85 (s, 6H), 1.18−1.10 (m, 18H). ^{31}P NMR ($CDCl_3$, ppm): δ 4.78 (J_{Pt-P} = 1549 Hz). ^{13}C NMR ($CDCl_3$, ppm): δ 151.7, 149.5, 144.4, 142.5, 139.5, 136.7, 128.3, 127.2, 126.0, 124.1, 124.0, 122.1, 118.5, 116.0, 98.1, 53.4, 17.2 (t, J_{C-P} = 19.0 Hz, CH_2P), 14.8 (CH_3), 14.4 (CH_3), 8.4 (CH_3CH_2P). IR (CH_2Cl_2): 2107 cm^{-1} (C≡C).

Physical Measurements. ^1H, ^{13}C, and ^{31}P NMR spectra were performed on a Bruker Avance III (400 MHz) spectrometer with $SiMe_4$ as the internal reference and H_3PO_4 as the external reference. UV−vis absorption spectra were measured on a Perkin-Elmer Lambda 25 UV−vis spectrophotometer. IR spectra were recorded on a Magna 750 FT-IR spectrophotometer. Elemental analyses (C, H, and N) were carried out on a Perkin-Elmer model 240 C elemental analyzer. Electrospray ionization mass spectrometry (ESI-MS) was recorded on a Finnigan DECAX-30000 LCQ mass spectrometer. UV light was produced using a ZF5 UV lamp (365 nm), and visible-light irradiation was carried out using a LZG220 V 1 kW tungsten lamp with cutoff filters. The quantum yields were determined by comparing the reaction yields of the diarylethenes relative to 1,2-bis(2-methyl-5-phenyl-3-thienyl)perfluorocyclopentene.[53] Cyclic voltammetry and differential pulse voltammetry were measured using a model 263A potentiostat/galvanostat in dichloromethane solutions containing 0.1 M $(Bu_4N)(PF_6)$ as the supporting electrolyte. Platinum and glassy graphite were used as the counter and working electrodes, respectively, and the potential was measured against the Ag/AgCl reference electrode.

Theoretical Methodology. All calculations of complexes **1oo**/**co**−**5oo**/**co** and **2cc**−**5cc** were implemented in the *Gaussian03* program package.[54] The DFT[55a] with the gradient-corrected correlation functional PBE1PBE[55b] was first used to optimize the geometrical structures in the ground states. In the optimization processes, the convergent values of maximum force, root-mean-square (rms) force, maximum displacement, and rms displacement were set by default. Then, 100 singlet excited states of these investigated complexes in a dichloromethane solution were calculated by the TD-DFT[56] method based on the optimized geometrical structures. The solvent effects were taken into account by the polarizable continuum model method.[57] The self-consistent-field convergence criteria of the rms density matrix and maximum density matrix were set at 10^{-8} and 10^{-6} au, respectively, in all of these electronic structure calculations. The iterations of excited states continued until the changes on the energies of states were no more than 10^{-7} au between iterations, and then convergences were reached in all of the excited states. In these calculations, the Lanl2dz effective core potential was used to describe the inner electrons of Pt, S, and P atoms, while its associated double-ζ basis set of Hay and Wadt was employed for the remaining outer electrons.[58] Other nonmetal atoms of F, N, C, and H were described by the all-electron basis set of 6-31G(p,d).[59] To precisely describe the molecular properties, one additional f-type polarization function was employed for the Pt atom (α_f = 0.18).[60] Visualization of the optimized structures and frontier molecular orbitals was performed by *GaussView*. The Ros and Schuit method (C-squared population analysis method)[61] was supported to analyze the partition orbital composition using the *Multiwfn2.4* program.[62]

■ ASSOCIATED CONTENT

Supporting Information

Tables and figures giving additional spectroscopic and computational data. This material is available free of charge via the Internet at http://pubs.acs.org.

AUTHOR INFORMATION

Corresponding Author

*E-mail: czn@fjirsm.ac.cn.

Notes

The authors declare no competing financial interest.

ACKNOWLEDGMENTS

We are grateful for financial support from the NSFC (Grants 20931006, U0934003, 91122006, and 21303204) the 973 project (2014CB845603) from MSTC and the NSF of Fujian Province (Grant 2011J01065).

REFERENCES

(1) (a) Irie, M. *Chem. Rev.* **2000**, *100*, 1685. (b) Tsujiokaa, T.; Irie, M. *J. Photochem. Photobiol., C* **2010**, *11*, 1.
(2) (a) Tian, H.; Yang, S. J. *Chem. Soc. Rev.* **2004**, *33*, 85. (b) Tian, H.; Feng, Y. *J. Mater. Chem.* **2008**, *18*, 1617.
(3) (a) Wenger, O. S. *Chem. Soc. Rev.* **2012**, *41*, 3772. (b) Yun, C.; You, J.; Kim, J.; Huh, J.; Kim, E. *J. Photochem. Photobiol., C* **2009**, *10*, 111. (c) Myles, A. J.; Branda, N. R. *Adv. Funct. Mater.* **2002**, *12*, 167. (d) Gust, D.; Andreasson, J.; Pischel, U.; Moore, T. A.; Moore, A. L. *Chem. Commun.* **2012**, *48*, 1947.
(4) Ko, C.-C.; Yam, V. W.-W. *J. Mater. Chem.* **2010**, *20*, 2063.
(5) Kume, S.; Nishihara, H. *Dalton Trans.* **2008**, 3260.
(6) Akita, M. *Organometallics* **2011**, *30*, 43.
(7) Hasegawa, Y.; Nakagawa, T.; Kawai, T. *Coord. Chem. Rev.* **2010**, *254*, 2643.
(8) Browne, W. R. *Coord. Chem. Rev.* **2008**, *252*, 2470.
(9) Guerchais, V.; Ordronneau, L.; Bozec, H. L. *Coord. Chem. Rev.* **2010**, *254*, 2533.
(10) Liu, Y.; Lagrost, C.; Costuas, K.; Tchouar, N.; Bozec, H. L.; Rigaut, S. *Chem. Commun.* **2008**, 6117.
(11) (a) Tanaka, Y.; Inagaki, A.; Akita, M. *Chem. Commun.* **2007**, 1169. (b) Tanaka, Y.; Ishisaka, T.; Inagaki, A.; Koike, T.; Lapinte, C.; Akita, M. *Chem.—Eur. J.* **2010**, *16*, 4762.
(12) (a) Chan, J. C.-H.; Lam, W. H.; Wong, H.-L.; Zhu, N.; Wong, W.-T.; Yam, V. W.-W. *J. Am. Chem. Soc.* **2011**, *133*, 12690. (b) Lee, P. H.-M.; Ko, C.-C.; Zhu, N.; Yam, V. W.-W. *J. Am. Chem. Soc.* **2007**, *129*, 6058.
(13) Morimoto, M.; Miyasaka, H.; Yamashita, M.; Irie, M. *J. Am. Chem. Soc.* **2009**, *131*, 9823.
(14) Ordronneau, L.; Nitadori, H.; Ledoux, I.; Singh, A.; Williams, J. A. G.; Akita, M.; Guerchais, V.; Bozec, H. L. *Inorg. Chem.* **2012**, *51*, 5627.
(15) He, B.; Wenger, O. S. *Inorg. Chem.* **2012**, *51*, 4335.
(16) Zhong, Y.-W.; Vila, N.; Henderson, J. C.; Flores-Torres, S.; Abruna, H. D. *Inorg. Chem.* **2007**, *46*, 10470.
(17) (a) Jukes, R. T. F.; Adamo, V.; Hartl, F.; Belser, P.; De Cola, L. *Inorg. Chem.* **2004**, *43*, 2779. (b) Fraysse, S.; Coudret, C.; Launay, J.-P. *Eur. J. Inorg. Chem.* **2000**, 1581.
(18) (a) Neilson, B. M.; Lynch, V. M.; Bielawski, C. W. *Angew. Chem., Int. Ed.* **2011**, *50*, 10322. (b) Neilson, B. M.; Bielawski, C. W. *J. Am. Chem. Soc.* **2012**, *134*, 12693.
(19) Lin, Y.; Yin, J.; Yuan, J.; Hu, M.; Li, Z.; Yu, G.-A.; Liu, S. H. *Organometallics* **2010**, *29*, 2808.
(20) Indelli, M. T.; Carli, S.; Ghirotti, M.; Chiorboli, C.; Ravaglia, M.; Garavelli, M.; Scandola, F. *J. Am. Chem. Soc.* **2008**, *130*, 7286.
(21) Roberts, M. N.; Nagle, J. K.; Majewski, M. B.; Finden, J. G.; Branda, N. R.; Wolf, M. O. *Inorg. Chem.* **2011**, *50*, 4956.
(22) (a) Uchida, K.; Yamanoi, Y.; Yonezawa, T.; Nishihara, H. *J. Am. Chem. Soc.* **2011**, *133*, 9239. (b) Green, K. A.; Cifuentes, M. P.; Corkery, T. C.; Samoc, M.; Humphrey, M. G. *Angew. Chem., Int. Ed.* **2009**, *48*, 7867.
(23) (a) Perrier, A.; Maurel, F.; Jacquemin, D. *Acc. Chem. Res.* **2012**, *45*, 1173. (b) Perrier, A.; Maurel, F.; Jacquemin, D. *J. Phys. Chem. C* **2011**, *115*, 9193. (c) Perrier, A.; Maurel, F.; Ciofini, I.; Jacquemin, D. *Chem. Phys. Lett.* **2011**, *502*, 77.
(24) (a) Kawai, T.; Sasakia, T.; Irie, M. *Chem. Commun.* **2001**, 711. (b) Kaieda, T.; Kobatake, S.; Miyasaka, H.; Murakami, M.; Iwai, N.; Nagata, Y.; Itaya, A.; Irie, M. *J. Am. Chem. Soc.* **2002**, *124*, 2105.
(25) (a) Peters, A.; Branda, N. R. *Adv. Mater. Opt. Electron.* **2000**, *10*, 245. (b) Wang, H.; Xu, W.; Zhu, D. *Tetrahedron* **2012**, *68*, 8719.
(26) (a) Areephong, J.; Hurenkamp, J. H.; Milder, M. T. W.; Meetsma, A.; Herek, J. L.; Browne, W. R.; Feringa, B. L. *Org. Lett.* **2009**, *11*, 721. (b) Liu, H.-h.; Chen, Y. *J. Mater. Chem.* **2011**, *21*, 1246.
(27) (a) Higashiguchi, K.; Matsuda, K.; Tanifuji, N.; Irie, M. *J. Am. Chem. Soc.* **2005**, *127*, 8922. (b) Higashiguchi, K.; Matsuda, K.; Irie, M. *Angew. Chem., Int. Ed.* **2003**, *42*, 3537.
(28) (a) Ko, C.-C.; Lam, W. H.; Yam, V. W.-W. *Chem. Commun.* **2008**, 5203. (b) Wong, H.-L.; Ko, C.-C.; Lam, W. H.; Zhu, N.; Yam, V. W.-W. *Chem.—Eur. J.* **2009**, *15*, 10005.
(29) Aubert, V.; Ishow, E.; Ibersiene, F.; Boucekkine, A.; Williams, J. A. G.; Toupet, L.; Metivier, R.; Nakatani, K.; Guerchais, V.; Le Bozec, H. *New J. Chem.* **2009**, *33*, 1320.
(30) Jung, I.; Choi, H.; Kim, E.; Lee, C.-H.; Kanga, S. O.; Ko, J. *Tetrahedron* **2005**, *61*, 12256.
(31) (a) Zhao, H.; Al-Atar, U.; Pace, T. C. S.; Bohne, C.; Branda, N. R. *J. Photochem. Photobiol., A* **2008**, *200*, 74. (b) Tian, H.; Chen, B.; Tu, H.; Mullen, K. *Adv. Mater.* **2002**, *14*, 918.
(32) (a) Yam, V. W.-W.; Lee, J. K.-W.; Ko, C.-C.; Zhu, N. *J. Am. Chem. Soc.* **2009**, *131*, 912. (b) Wong, H.-L.; Tao, C.-H.; Zhu, N.; Yam, V. W.-W. *Inorg. Chem.* **2011**, *50*, 471.
(33) Shilova, E. A.; Heynderickx, A.; Siri, O. *J. Org. Chem.* **2010**, *75*, 1855.
(34) Areephong, J.; Logtenberg, H.; Browne, W. R.; Feringa, B. L. *Org. Lett.* **2010**, *12*, 2132.
(35) Tan, W.; Li, X.; Zhang, J.; Tian, H. *Dyes Pigm.* **2011**, *89*, 260.
(36) (a) Kobatake, S.; Kuma, S.; Irie, M. *J. Phys. Org. Chem.* **2007**, *20*, 960. (b) Kobatake, S.; Kuma, S.; Irie, M. *Bull. Chem. Soc. Jpn.* **2004**, *77*, 945.
(37) Zhong, Y.-W.; Vila, N.; Henderson, J. C.; Abruna, H. D. *Inorg. Chem.* **2009**, *48*, 7080.
(38) Hervault, Y.-M.; Ndiaye, C. M.; Norel, L.; Lagrost, C.; Rigaut, S. *Org. Lett.* **2012**, *14*, 4454.
(39) Kim, H. J.; Jang, J. H.; Choi, H.; Lee, T.; Ko, J.; Yoon, M.; Kim, H.-J. *Inorg. Chem.* **2008**, *47*, 2411.
(40) Chen, S.; Chen, L.-J.; Yang, H.-B.; Tian, H.; Zhu, W. *J. Am. Chem. Soc.* **2012**, *134*, 13596.
(41) (a) Matsuda, K.; Irie, M. *J. Am. Chem. Soc.* **2001**, *123*, 9896. (b) Kobatake, S.; Irie, M. *Tetrahedron* **2003**, *59*, 8359.
(42) Areephong, J.; Browne, W. R.; Feringa, B. L. *Org. Biomol. Chem.* **2007**, *5*, 1170.
(43) (a) Choi, H.; Jung, I.; Song, K. H.; Song, K.; Shin, D.-S.; Kang, S. O.; Ko, J. *Tetrahedron* **2006**, *62*, 9059. (b) Ordronneau, L.; Aubert, V.; Metivier, R.; Ishow, E.; Boixel, J.; Nakatani, K.; Ibersiene, F.; Hammoutene, D.; Boucekkine, A.; Le Bozeca, H.; Guerchais, V. *Phys. Chem. Chem. Phys.* **2012**, *14*, 2599.
(44) Li, B.; Wu, Y.-H.; Wen, H.-M.; Shi, L.-X.; Chen, Z.-N. *Inorg. Chem.* **2012**, *51*, 1933.
(45) (a) Roberts, M. N.; Carling, C.-J.; Nagle, J. K.; Branda, N. R.; Wolf, M. O. *J. Am. Chem. Soc.* **2009**, *131*, 16644.
(46) Li, B.; Wang, J.-Y.; Wen, H.-M.; Shi, L.-X.; Chen, Z.-N. *J. Am. Chem. Soc.* **2012**, *134*, 16059.
(47) (a) Uchida, K.; Irie, M. *Chem. Lett.* **1995**, 969. (b) Uchida, K.; Matsuoka, T.; Kobatake, S.; Yamaguchi, T.; Irie, M. *Tetrahedron* **2001**, *57*, 4559.
(48) (a) He, B.; Wenger, O. S. *J. Am. Chem. Soc.* **2011**, *133*, 17027. (b) Reuter, L. G.; Bonn, A. G.; Stuckl, A. C.; He, B.; Pati, P. B.; Zade, S. S.; Wenger, O. S. *J. Phys. Chem. A* **2012**, *116*, 7345.
(49) Diez, A.; Fernandez, J.; Lalinde, E.; Moreno, M. T.; Sanchez, S. *Dalton Trans.* **2008**, 4926.
(50) Osella, D.; Gobetto, R.; Nervi, C.; Ravera, M.; D'Amato, R.; Russo, M. V. *Inorg. Chem. Commun.* **1998**, *1*, 239.
(51) (a) Kauffman, G. B.; Teter, L. A. *Inorg. Synth.* **1963**, *7*, 245. (b) Pu, S.; Fan, C.; Miao, W.; Liu, G. *Dyes Pigm.* **2010**, *84*, 25.

(52) Sun, F.; Zhang, F. S.; Guo, H. B.; Zhou, X. H.; Wang, R. J.; Zhao, F. Q. *Tetrahedron* **2003**, *59*, 7615.
(53) Irie, M.; Lifka, T.; Kobatake, S.; Kato, N. *J. Am. Chem. Soc.* **2000**, *122*, 4871.
(54) Frisch, M. J.; Trucks, G. W.; Schlegel, H. B.; Scuseria, G. E.; Robb, M. A.; Cheeseman, J. R.; Montgomery, J. A., Jr.; Vreven, T.; Kudin, K. N.; Burant, J. C.; Millam, J. M.; Iyengar, S. S.; Tomasi, J.; Barone, V.; Mennucci, B.; Cossi, M.; Scalmani, G.; Rega, N.; Petersson, G. A.; Nakatsuji, H.; Hada, M.; Ehara, M.; Toyota, K.; Fukuda, R.; Hasegawa, J.; Ishida, M.; Nakajima, T.; Honda, Y.; Kitao, O.; Nakai, H.; Klene, M.; Li, X.; Knox, J. E.; Hratchian, H. P.; Cross, J. B.; Bakken, V.; Adamo, C.; Jaramillo, J.; Gomperts, R.; Stratmann, R. E.; Yazyev, O.; Austin, A. J.; Cammi, R.; Pomelli, C.; Ochterski, J. W.; Ayala, P. Y.; Morokuma, K.; Voth, G. A.; Salvador, P.; Dannenberg, J. J.; Zakrzewski, V. G.; Dapprich, S.; Daniels, A. D.; Strain, M. C.; Farkas, O.; Malick, D. K.; Rabuck, A. D.; Raghavachari, K.; Foresman, J. B.; Ortiz, J. V.; Cui, Q.; Baboul, A. G.; Clifford, S.; Cioslowski, J.; Stefanov, B. B.; Liu, G.; Liashenko, A.; Piskorz, P.; Komaromi, I.; Martin, R. L.; Fox, D. J.; Keith, T.; Al-Laham, M. A.; Peng, C. Y.; Nanayakkara, A.; Challacombe, M.; Gill, P. M. W.; Johnson, B.; Chen, W.; Wong, M. W.; Gonzalez, C.; Pople, J. A. *Gaussian03*, revision D.02; Gaussian, Inc.: Wallingford, CT, 2004.
(55) (a) Becke, A. D. *J. Chem. Phys.* **1993**, *98*, 5648. (b) Perdew, J. P.; Burke, K.; Ernzerhof, M. *Phys. Rev. Lett.* **1996**, *77*, 3865.
(56) (a) Bauernschmitt, R.; Ahlrichs, R. *Chem. Phys. Lett.* **1996**, *256*, 454. (b) Casida, M. E.; Jamorski, C.; Casida, K. C.; Salahub, D. R. *J. Chem. Phys.* **1998**, *108*, 4439.
(57) (a) Barone, V.; Cossi, M.; Tomasi, J. *J. Chem. Phys.* **1997**, *107*, 3210. (b) Cossi, M.; Scalmani, G.; Rega, N.; Barone, V. *J. Chem. Phys.* **2002**, *117*, 43.
(58) (a) Hay, P. J.; Wadt, W. R. *J. Chem. Phys.* **1985**, *82*, 270. (b) Wadt, W. R.; Hay, P. J. *J. Chem. Phys.* **1985**, *82*, 284. (c) Hay, P. J.; Wadt, W. R. *J. Chem. Phys.* **1985**, *82*, 299.
(59) Francl, M. M.; Pietro, W. J.; Hehre, W. J.; Binkley, J. S.; Gordon, M. S.; DeFrees, D. J.; Pople, J. A. *J. Chem. Phys.* **1982**, *77*, 3654.
(60) Pyykkö, P.; Runeberg, N.; Mendizabal, F. *Chem.—Eur. J.* **1997**, *3*, 1451.
(61) Ros, P.; Schuit, G. C. A. *Theor. Chim. Acta* **1966**, *4*, 1.
(62) Lu, T.; Chen, F. W. *J. Comput. Chem.* **2012**, *33*, 580.